InSAR observations of syn-seismic slip on faults due to M∼6 earthquakes

Henriette Sudhaus, John Begg, Vasiliki Mousopoulou, Julia Knüppel and Tilman May

More Info / Details: Mousopoulou et al. (2022) and talk supplement

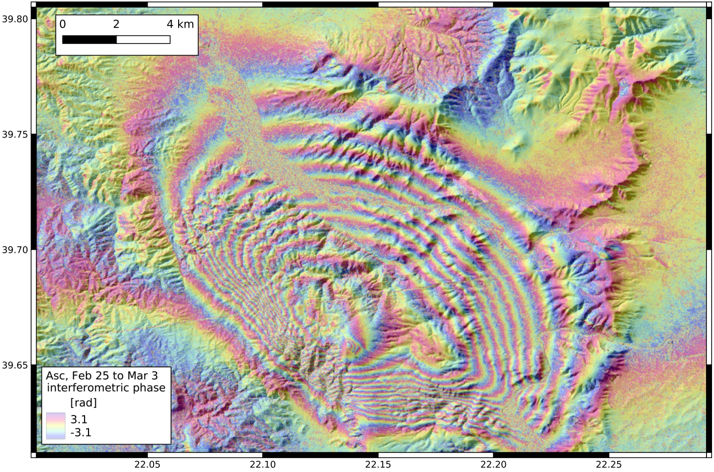

Tyrnavos earthquake Mw6.3, on Mar 3 2020 (Greece)

Sentinel-1 interferogram spanning 6 days

InSAR observations of syn-seismic slip on faults due to M∼6 earthquakes

Henriette Sudhaus, John Begg, Vasiliki Mousopoulou, Julia Knüppel and Tilman May

More Info / Details: ➽ Mousopoulou et al. (2022) and talk supplement

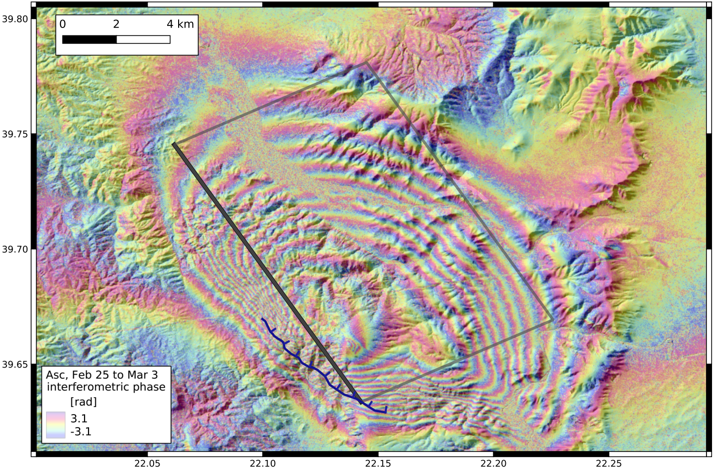

Tyrnavos earthquake Mw6.3, on Mar 3 2020 (Greece)

Sentinel-1 interferogram spanning 6 days

∃ coseism. surface rupture

☐ fault model projection

InSAR observations of syn-seismic slip on faults due to M∼6 earthquakes

Henriette Sudhaus, John Begg, Vasiliki Mousopoulou, Julia Knüppel and Tilman May

More Info / Details: Mousopoulou et al. (2022) and talk supplement

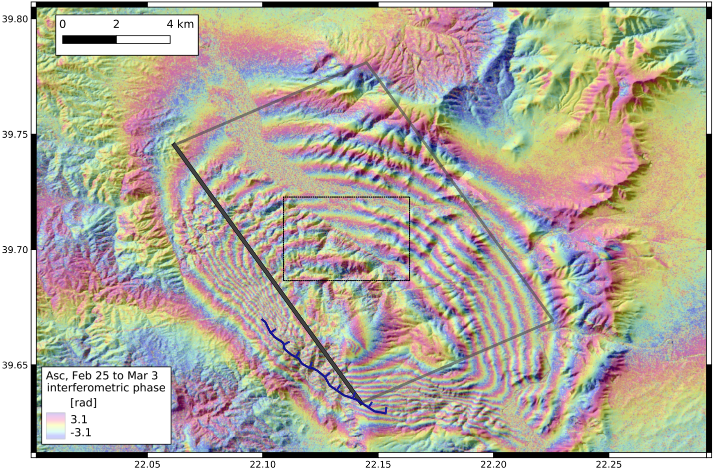

Tyrnavos earthquake Mw6.3, on Mar 3 2020 (Greece)

Sentinel-1 interferogram spanning 6 days

∃ coseism. surface rupture

☐ fault model projection

Observations of synseismic fault activation

observed character: small slip along kilometers of pre-existing faults

Coseismic differential interferogram (unfiltered)

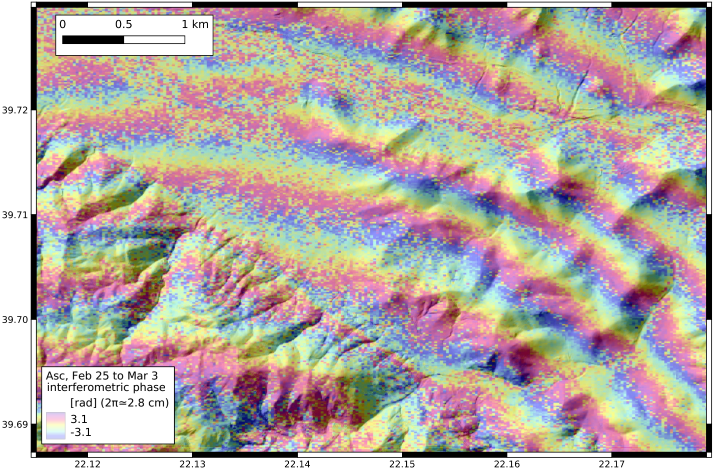

phase jumps of ∼1 cm
linear along kilometers
slip direction varies

Observations of synseismic fault activation

observed character: small slip along kilometers of pre-existing faults

Coseismic displacement. Up component (inferred from asc & dsc acquisitions)

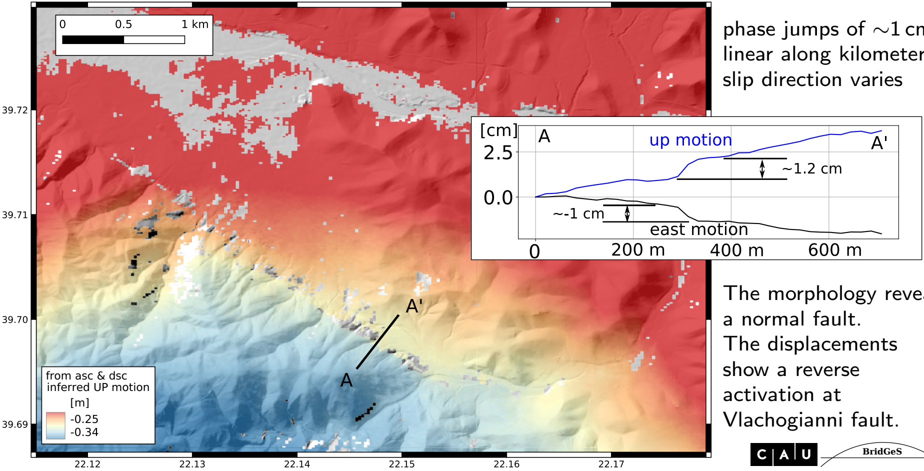

phase jumps of ∼1 cm
linear along kilometers
slip direction varies

The morphology reveals a normal fault.
The displacements show a reverse activation at Vlachogianni fault.

Analysis of synseismic fault activation

Slip direction varies spatially. It sometimes flips along the same fault.

Mapping of synseismic fault activations

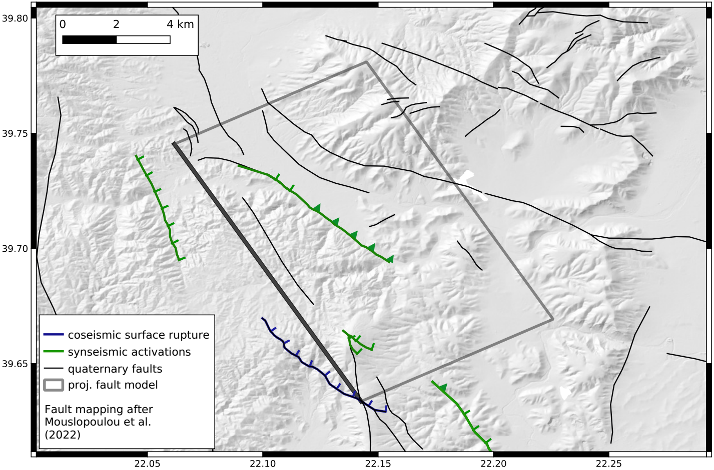

Normal and reverse faulting seems to prevail.

Any north components are only weakly projected in InSAR imagery and might be missed.

Is there a relationship of fault motion and coseismic stress change?

Estimating the coseismic surface strain field

based on the fault model of an optimization

3D strain vector in east and north direction only, because the displacements are not continuous across the free surface.

$$\epsilon = \begin{pmatrix} \frac{\partial E}{\partial e} & \frac{\partial E}{\partial n} & \frac{\partial E}{\partial u} \\ \frac{\partial N}{\partial e} & \frac{\partial N}{\partial n} & \frac{\partial N}{\partial u} \\ \frac{\partial U}{\partial e} & \frac{\partial U}{\partial n} & \frac{\partial U}{\partial u} \end{pmatrix} = \begin{pmatrix} \epsilon_{ee} & \epsilon_{en} & \epsilon_{eu} \\ \epsilon_{ne} & \epsilon_{nn} & \epsilon_{nu} \\ \epsilon_{ue} & \epsilon_{un} & \epsilon_{uu} \end{pmatrix},$$

with the 2^{nd} strain invariant $= \epsilon_{ee} \cdot \epsilon_{nn} - (\frac{1}{2}(\epsilon_{en} + \epsilon_{ne}))^2$

A positive 2nd strain invariant shows a surface under compression.
A negative 2nd strain invariant shows a surface under extension.

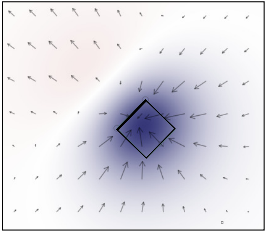

surface displacements ENU

Fault activation w.r.t. coseismic strain

Slip direction in relationship with earthquake-induced surface strain

A positive 2nd strain invariant shows a surface under compression.

A negative 2nd strain invariant shows a surface under extension.

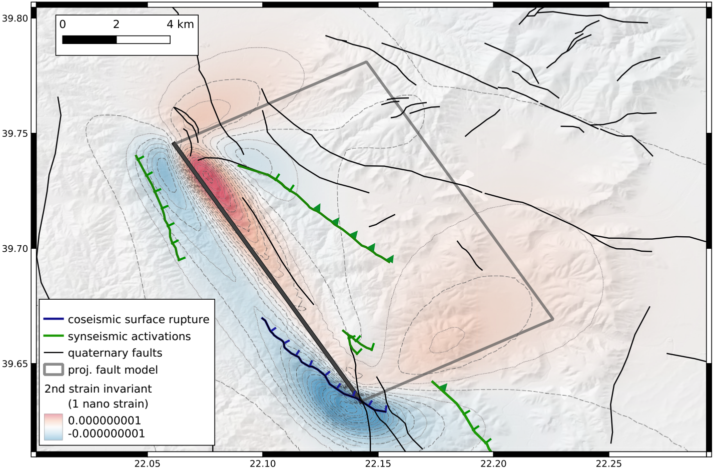

Normal and reverse faulting indeed follow the strain regime pattern imposed by the earthquake.

Small deviation from that rule may stem from model simplifications:

- rectangular fault with uniform slip
- horizontally layered medium

Fault activation w.r.t. coseismic strain

Slip direction in relationship with earthquake-induced surface strain

A positive 2nd strain invariant shows a surface under compression.

A negative 2nd strain invariant shows a surface under extension.

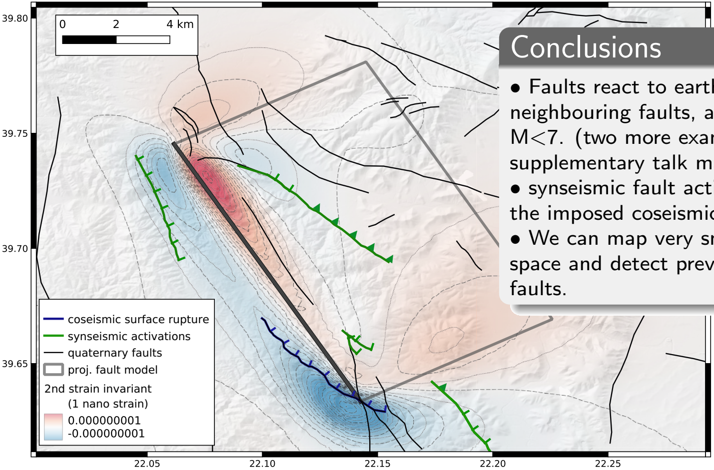

Conclusions

- Faults react to earthquakes at neighbouring faults, also for earthquakes M<7. (two more examples online in the supplementary talk material)
- synseismic fault activation releases part of the imposed coseismic stress.
- We can map very small fault slips from space and detect previously unmapped faults.

Anything else to learn?

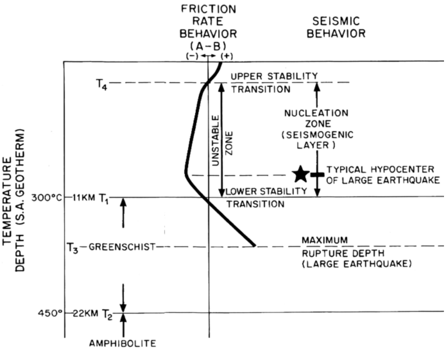

graphic: Scholz 2002

We know:
At shallow depth the friction law realizes velocity strengthening.

Effects:

- earthquakes do not nucleate at shallow depth
- ruptures slow down near the surface
- surface-breaking earthquakes most often show a slip deficit at shallow depth

Questions:
When and how is permanent surface strain realized?

Does syn-seismic slip play a role in the tectonic stress release at shallow depth?
We think yes, even though it may be a small role.

Three “ordinary“ normal-faulting earthquakes

Analysing the surface strain field

based on displacement maps, here observed with InSAR

strain vector at surface:

$$\epsilon = \begin{pmatrix} \epsilon_{ee} & \epsilon_{en} & \epsilon_{eu} \\ \epsilon_{ne} & \epsilon_{nn} & \epsilon_{nu} \\ \epsilon_{ue} & \epsilon_{un} & \epsilon_{uu} \end{pmatrix}$$

surface displacements ENU

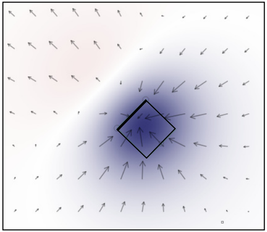

strain vector from InSAR observations (basically no north):

$$\epsilon = \begin{pmatrix} \epsilon_{ee} & \epsilon_{en} & \epsilon_{eu} \\ \epsilon_{ne} & \epsilon_{nn} & \epsilon_{nu} \\ \epsilon_{(u+n)e} & \epsilon_{(u+n)n} & \epsilon_{(u+n)u} \end{pmatrix}$$

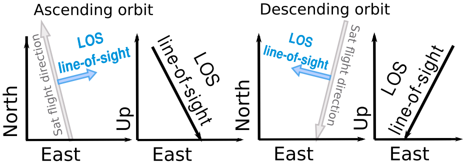

predicted coseismic strain vector at surface, based on a fault model:

$$\epsilon = \begin{pmatrix} \epsilon_{ee} & \epsilon_{en} & \epsilon_{eu} \\ \epsilon_{ne} & \epsilon_{nn} & \epsilon_{nu} \\ \epsilon_{ue} & \epsilon_{un} & \epsilon_{uu} \end{pmatrix}$$, with the 2^{nd} strain invariant $= \epsilon_{ee} \cdot \epsilon_{nn} - (\frac{1}{2}(\epsilon_{en} + \epsilon_{ne}))^2$

A Mw6.3 earthquake in Xizang, Tibet

on July 22 in 2020

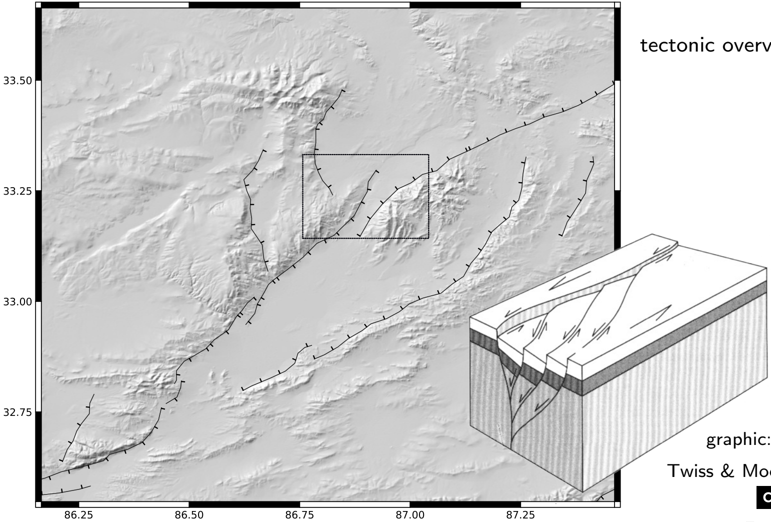

tectonic overview

negative flower structure

graphic:

Twiss & Moores (1992)

A Mw6.3 earthquake in Xizang, Tibet

on July 22 in 2020

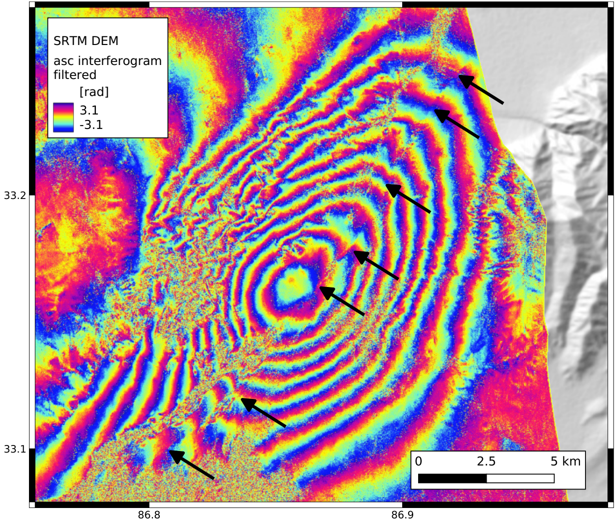

arrows point to surface rupture.

A Mw6.3 earthquake in Xizang, Tibet

on July 22 in 2020, InSAR strain maps used for mapping strain localization

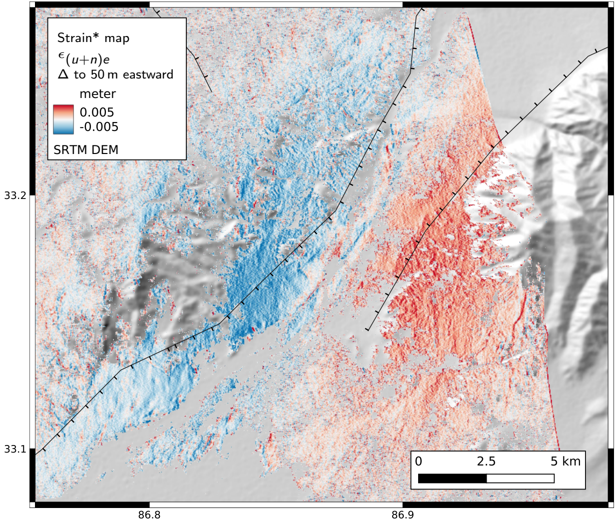

shown strain component:

$$\epsilon = \begin{pmatrix} \epsilon_{ee} & \epsilon_{en} \\ \epsilon_{ne} & \epsilon_{nn} \\ \boldsymbol{\epsilon_{(u+n)e}} & \epsilon_{(u+n)n} \end{pmatrix}$$

blue linear features:
east-side goes down
red linear features:
east-side goes up

A Mw6.3 earthquake in Xizang, Tibet

on July 22 in 2020, InSAR strain maps used for mapping strain localization

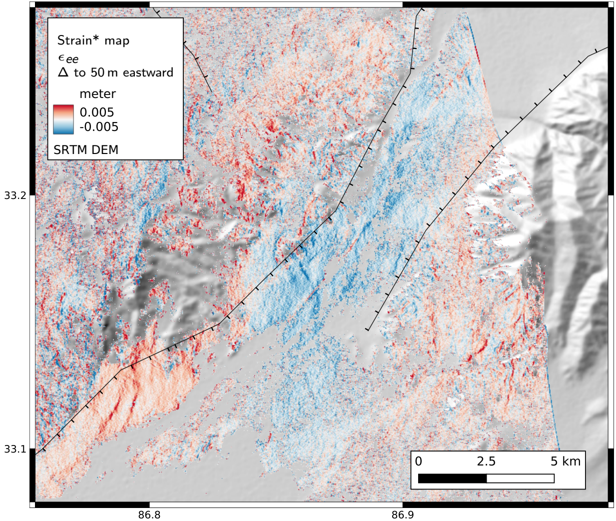

shown component:

$$\epsilon = \begin{pmatrix} \epsilon_{ee} & \epsilon_{en} \\ \epsilon_{ne} & \epsilon_{nn} \\ \epsilon_{(u+n)e} & \epsilon_{(u+n)n} \end{pmatrix}$$

blue linear features:
east-side goes west

red linear features:
east-side goes east

A Mw6.3 earthquake in Xizang, Tibet

on July 22 in 2020, InSAR strain maps used for mapping strain localization

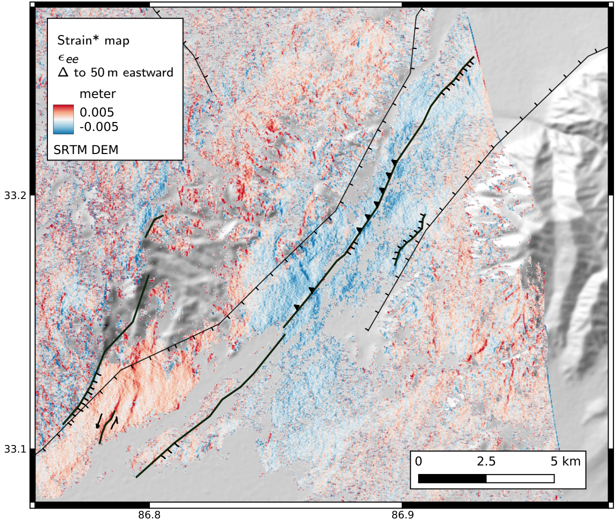

shown component:

$$\epsilon = \begin{pmatrix} \epsilon_{ee} & \epsilon_{en} \\ \epsilon_{ne} & \epsilon_{nn} \\ \epsilon_{(u+n)e} & \epsilon_{(u+n)n} \end{pmatrix}$$

blue linear features:
east-side goes west

red linear features:
east-side goes east

A Mw6.3 earthquake in Xizang, Tibet

on July 22 in 2020, predicted strain versus mapped slip directions

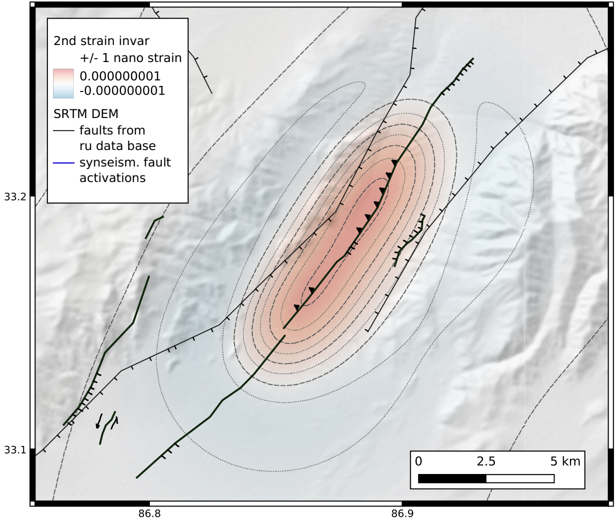

predicted strain:

$$\epsilon = \begin{pmatrix} \epsilon_{ee} & \epsilon_{en} \\ \epsilon_{ne} & \epsilon_{nn} \\ \epsilon_{ue} & \epsilon_{un} \end{pmatrix}$$

2n invariant:

$$\epsilon_{ee} \cdot \epsilon_{nn} - (\tfrac{1}{2}(\epsilon_{en} + \epsilon_{ne}))^2$$

blue area: extension

red area: compression

strain predictions based on rupture modeling by L. Diefenbacher

Mw6.0 Arkalochori earthquake in central Crete

on September 27 2021

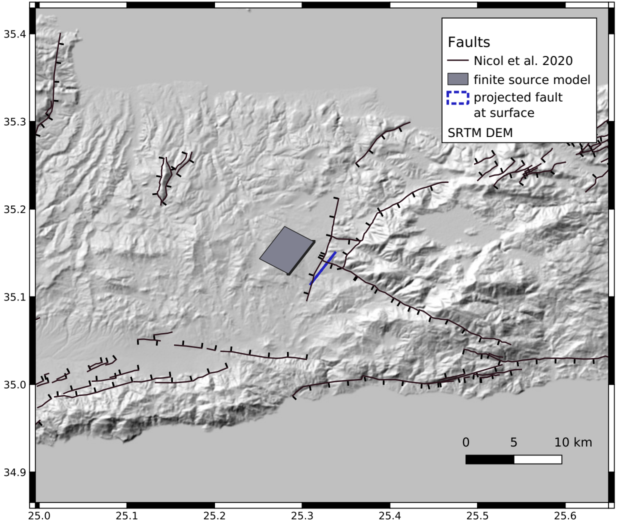

tectonic overview

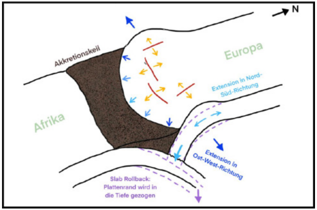

sketched extensional regime

Faults after Nicol et al. (2020)
graphic and fault modelling:
J. Knüppel (2022)

Mw6.0 Arkalochori earthquake in central Crete

on September 27 2021

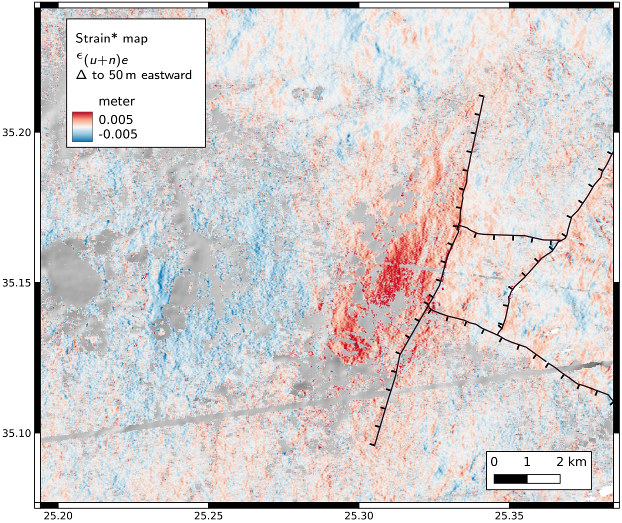

shown strain component:

$$\epsilon = \begin{pmatrix} \epsilon_{ee} & \epsilon_{en} \\ \epsilon_{ne} & \epsilon_{nn} \\ \boldsymbol{\epsilon_{(u+n)e}} & \epsilon_{(u+n)n} \end{pmatrix}$$

blue linear features:
east-side goes down
red linear features:
east-side goes up

Faults after Nicol et al. (2020)

Mw6.0 Arkalochori earthquake in central Crete

on September 27 2021

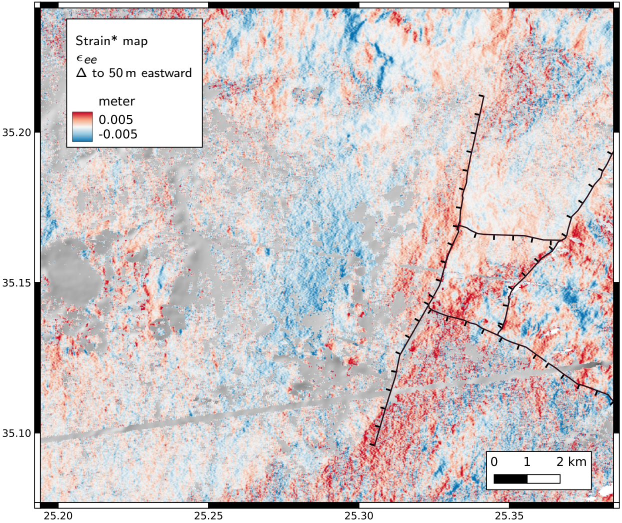

shown component:

$$\epsilon = \begin{pmatrix} \epsilon_{ee} & \epsilon_{en} \\ \epsilon_{ne} & \epsilon_{nn} \\ \epsilon_{(u+n)e} & \epsilon_{(u+n)n} \end{pmatrix}$$

blue linear features:
east-side goes west
red linear features:
east-side goes east

Faults after Nicol et al. (2020)

Mw6.0 Arkalochori earthquake in central Crete

on September 27 2021

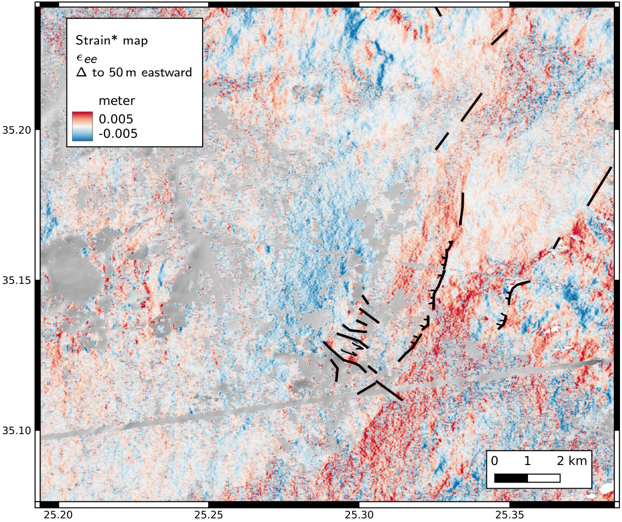

shown component:

$$\epsilon = \begin{pmatrix} \epsilon_{ee} & \epsilon_{en} \\ \epsilon_{ne} & \epsilon_{nn} \\ \epsilon_{(u+n)e} & \epsilon_{(u+n)n} \end{pmatrix}$$

blue linear features:
east-side goes west

red linear features:
east-side goes east

Fault detection by J. Knüppel

Mw6.0 Arkalochori earthquake in central Crete

on September 27 2021

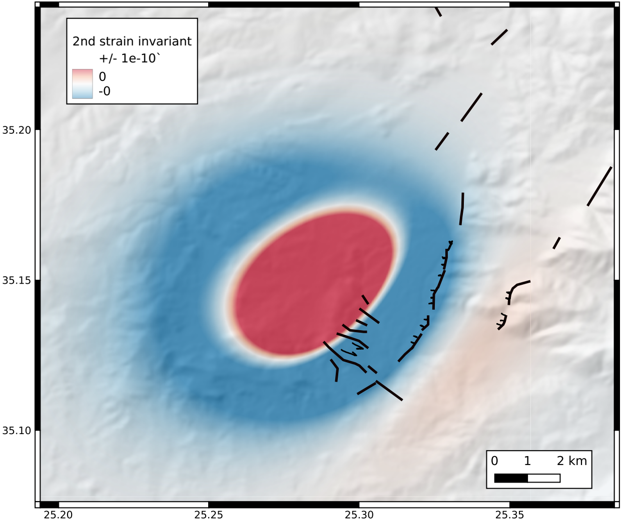

predicted strain:

$$\epsilon = \begin{pmatrix} \epsilon_{ee} & \epsilon_{en} \\ \epsilon_{ne} & \epsilon_{nn} \\ \epsilon_{ue} & \epsilon_{un} \end{pmatrix}$$

2n invariant:

$$\epsilon_{ee} \cdot \epsilon_{nn} - (\frac{1}{2}(\epsilon_{en} + \epsilon_{ne}))^2$$

blue area: extension

red area: compression

rupture modeling by J. Knüppel

CAU BridGeS

Mw6.0 Arkalochori earthquake in central Crete

on September 27 2021

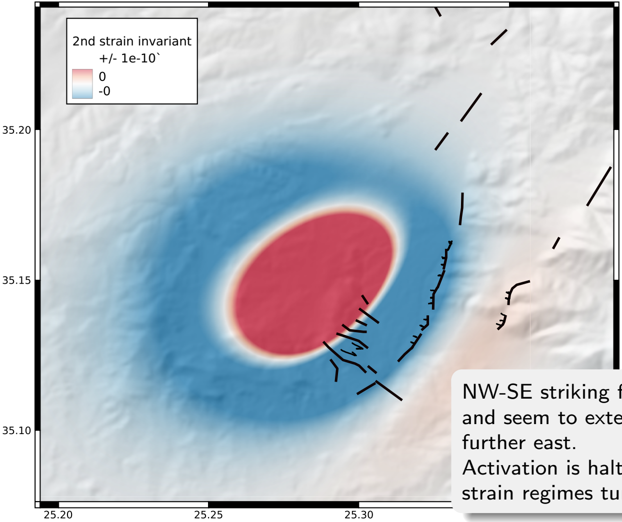

predicted strain:

$$\epsilon = \begin{pmatrix} \epsilon_{ee} & \epsilon_{en} \\ \epsilon_{ne} & \epsilon_{nn} \\ \epsilon_{ue} & \epsilon_{un} \end{pmatrix}$$

2n invariant:

$$\epsilon_{ee} \cdot \epsilon_{nn} - \left(\frac{1}{2}(\epsilon_{en} + \epsilon_{ne})\right)^2$$

blue area: extension

red area: compression

rupture modeling by J. Knüppel

NW-SE striking faults are newly detected and seem to extend from exposed faults further east.
Activation is halted in the west, where strain regimes turns to compression.